

PERFORMANCE ANALYSIS OF SOLAR AIR HEATING DUCTS ON THE ABSORBER PLATE USING CFD WITH VARIOUS TYPES OF RIBS

Prof. Pushparaj Singh*¹, Prof. Amol Kumar Tripathi*², Vipin Kumar Shukla*³

*^{1,2}Rewa Institute of Technology, Assistant Professor, Rewa, MP, India.

*³Rewa Institute of Technology, M.Tech Scholar, Rewa, MP, India.

ABSTRACT

Present work aimed at exploring different aspects of artificial roughness geometry in solar air heaters. A study of various rib shapes with different specifications reveals that artificial roughness contributes to an improved transfer of heat. In this present work, a 3-dimensional CFD analysis has been carried out to study heat transfer and fluid flow behavior in a rectangular duct of a solar air heater with one roughened wall having square and x-shaped rib roughness. The simulation programme ANSYS 14.5 was used for study of the heat transfer physiognomies of a rectangular duct of a solar air heater. The solar air heater with X-sectioned rib roughness on the absorber plate has been found to yield improved results relative to the square sectioned transverse rib and can thus be used to increase the heat transfer. The maximum enhancement in Nusselt number is found to be in X-shaped ribs, which is 1.109 times that of square ribs corresponding to at a Reynolds number of 15,000 for the investigated range of parameters.

Keywords: Artificial roughness, shape of rib, solar air heater, heat transfer, friction factor, and CFD.

I. INTRODUCTION

Thermo-hydraulic efficiency of any device depends on the configuration of the flow path and how the fluid interacts with the heated surfaces within the passageway. The performance of the solar air heating system depends largely on the configuration of the absorber plate and the flow-through duct [1, 2]. This is why many researchers have based their study on different aspects of the SAH structures, primarily the absorber plate and the duct incorporated with different shapes of ribs or turbulators, such as circular and square cross-section ribs, tapered rectangular cross-sections, various combinations of V-shaped ribs, wavy delta winglets, anchor-shaped inserts, perforated winglet vortex generators, etc.

With the energy generation costs through the use of non-renewable fuel resources, such as coal, crude oil, etc., and due to their limited stock and non-renewable nature, it has become necessary to develop effective designs for devices that use renewable energy sources such as solar energy [3]. Since flat plate SAH is commonly used in many domestic and industrial applications such as room heating, agricultural crop drying, desalination and other heating applications, improving designs for better thermal efficiency will make a major contribution to our increasing energy needs.

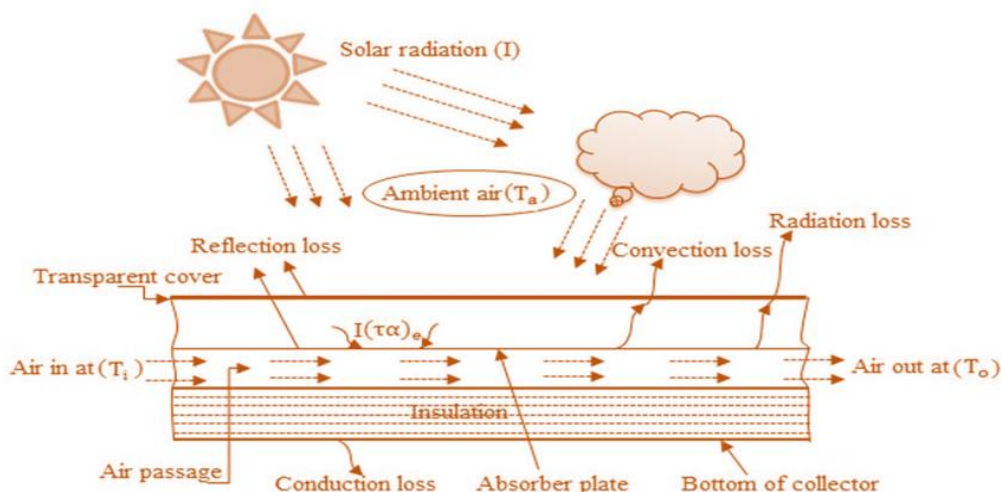


Fig.-1: Schematic diagram of conventional solar air heaters.

Moreover, if the availability of solar insolation is just around 4–6 hours a day, the SAH must be thermally efficient in order to allow use of the full portion of usable solar energy. There are two important facets of the SAH design: the absorber plate and the flow duct, where cold air enters, produces energy from the heated plate and escapes the passage [4]. The use of ribs or grooves on the inner surface of the heat exchangers was one of the regular passive approaches to break down the laminar sub-layer and create a turbulent local wall due to the isolation of the flow and the reattachment between the successive corrugation, which decreases thermal resistance and increases the heat transfer rate [5, 6].

In this present work a three dimensional CFD analysis was carried out in a rectangular duct of a solar air heater with a roughened wall having square and x-shape rib ruggedness to investigate the heat transfer and flow behaviour. The simulation programme ANSYS 14.5 was used for study of the heat transfer physiognomies of a rectangular duct of a solar air heater.

The main objective of the present studies is:

- The effect of roughness and flow parameters (square and 'x' section) rib on the absorber plate on average heat transfer and flow friction properties of artificial rugged solar air heaters.
- To figure out the optimum transverse rib configuration for heat transfer enhancement.
- Investigate the effect of roughness parameters on different SAH thermal properties, such as the number of Reynolds, the number of Nusselt, the coefficient of heat transfer and the flow friction factor, and compare the result with the smooth plate.
- To evaluate numerically and research the results of various rib shapes (square and 'x' section), organized in-line by a transversely ribbed rectangular solar air heater on the properties of thermal and fluid movement in turbulent flow.
- To research the results of various rib heights in order to identify the ideal geometry with the maximum performance assessment criteria (PEC) index.

II. CFD SIMULATION

The study uses the CFD model in this section to investigate the heat transfer physiognomies of an artificially roughened solar air heater, with effect of different ribs shapes mounted on the absorber plate. CFD review involves three major steps. The first step includes the creation of the geometry and mesh generation of the desired model, while the results are seen as expected in the last step. In the execution of the solver (middle) stage, the boundary conditions are fed into the model.

2.1. Geometrical details of computational model

The geometry for conducting simulation study is drawn from **Anil Singh Yadav and J.L. Bhagoria (2017) [6]**, a research scholar with exact sizes. The details of the geometry and computational model of conventional design are shown in Table 1 and Figure 2, and 3 respectively.

Table-1: Geometric parameters of Solar air Heater

Geometrical parameters	Value / Range
Test length of duct, L_2 (mm)	280
Entrance length of duct L_1 (mm)	245
Exit length of duct L_3 (mm)	115
Duct height, H (mm)	20
Duct width, W (mm)	100
Duct hydraulic diameter, D_h (mm)	33.33
Aspect ratio of duct, W/H (mm)	5
Rib height e (mm)	1.4

Pitch P (mm)	10
Relative roughness pitch, 'P/e'	7.14
Relative roughness height, 'e/D'	0.042

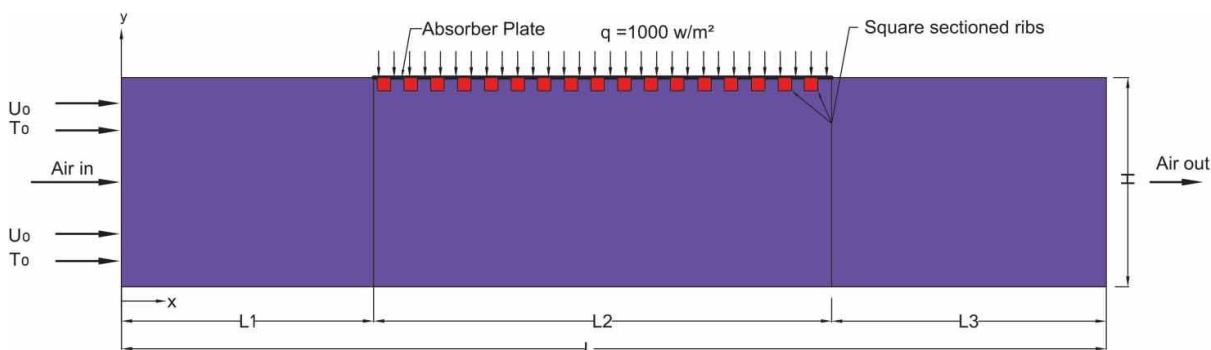


Fig.-2: Schematic of 2D computational domain.

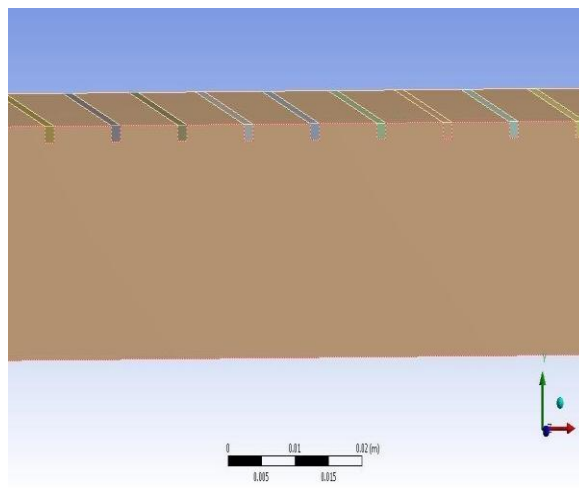
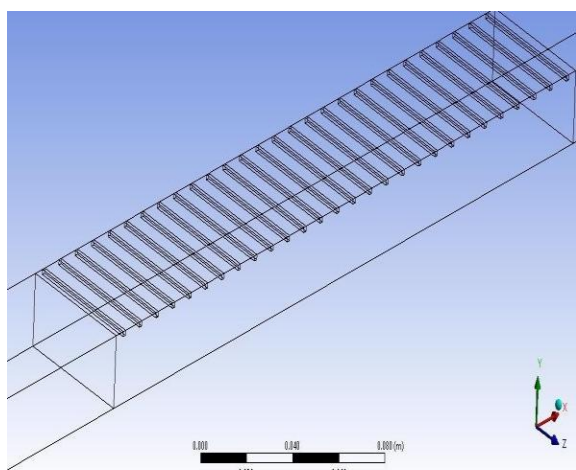


Fig.-3: Square shaped rib on the absorber plate of SAH (Conventional design).

After than in the proposed designs, 'x' section rib is employed on the absorber plate. The part of the model designed in ANSYS (fluent) workbench 14.5 software.

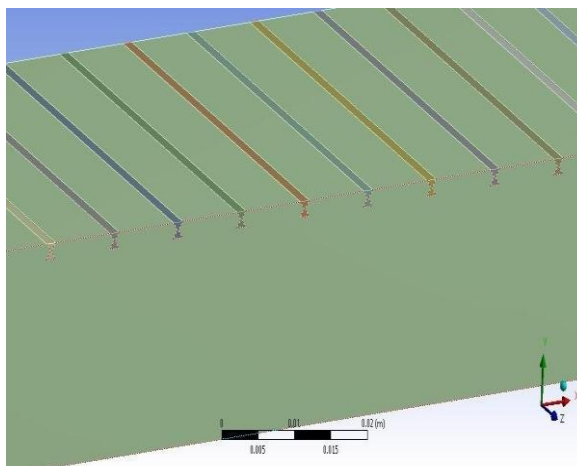
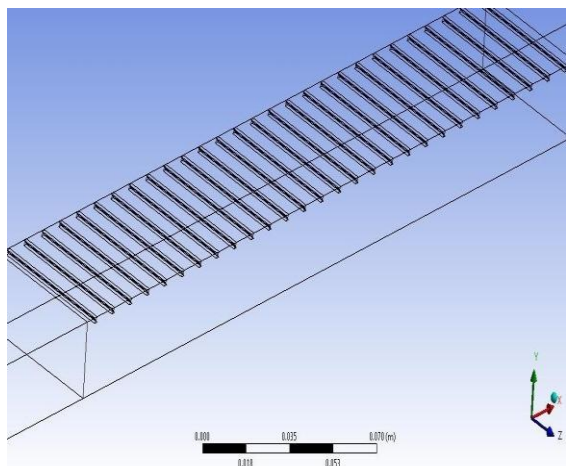


Fig.-4: X- shaped rib on the absorber plate of SAH(Proposed design).

2.2. Meshing

In the pre-processor step of ANSYS FLUENT R 14.5, a three-dimensional discretized model was developed. Although the styles of grids are connected to simulation performance, the entire structure is discretized in the finite volume by, default; a coarse mesh is generated by ANSYS software. Mesh contains mixed cells per unit area (ICEM Tetrahedral cells) having triangular faces at the boundaries. The meshing that has used in this analysis is mesh metric with medium smooth curvature.

Table-2: Meshing detail of various models

S. No.	Parameters	Square-shaped rib (Conventional design)	X-shaped rib (Proposed design)
1	Curvature	On	On
2	Smooth	Medium	Medium
3	Number of nodes	116843	119876
4	Number of elements	301265	311343
5	Mesh metric	None	None
6	Meshing type	Tetrahedral	Tetrahedral

2.3. Model Selection and Solution Methods

The RNG k-ε model was chosen as the turbulence model for the further study of the problem because the flow is turbulent. As a heat transfer model, the energy equation is also kept ON.

The numerical model for fluid flow and heat transfer through an artificially roughened solar air heater is developed under the following assumptions:

- The fluids sustain a single-phase, turbulent flow through the duct.
- 2D steady heat transfer fluid flow.
- Flow thoroughly formed both thermally and hydraulically (steady-state conditions).
- Both the fluid (air) and rigid absorber (aluminium) have continuous thermo-physical characteristics (temperature independent).
- Refused heat transfer by radiation.

The heat transfer equations and fluid flow structure contains the mass, momentum and energy conservation equation. The equations are as follows:

The mass conservation:

$$\frac{\partial(\rho u_i)}{\partial x_i} = 0$$

The momentum conservation:

$$\frac{\partial(\rho \bar{u}_i \bar{u}_j)}{\partial x_j} = -\frac{\partial \bar{P}}{\partial x_i} + \frac{\partial \left(\mu + \mu_t \left(\frac{\partial \bar{u}_i}{\partial x_j} + \frac{\partial \bar{u}_j}{\partial x_i} \right) \right)}{\partial x_j}$$

The energy conservation:

$$C_p \bar{u}_i \frac{\partial(\rho \bar{T})}{\partial x_i} = \frac{\partial \left(\lambda \frac{\partial \bar{T}}{\partial x_i} \right)}{\partial x_i} - C_p \frac{\partial \left(\frac{\mu_t}{Pr_t} \frac{\partial \bar{T}}{\partial x_i} \right)}{\partial x_i}$$

All governing equations are discretized by a second-order upwind-biased scheme using a finite volume approach and then solved in a segregated manner. The SIMPLE algorithm to couple pressure and velocity is selected for the incompressible flow computation. Convergence criteria are defined as 0.001 for all dependent variables. Whenever issues of integration are found, the solution starts with the upwind discretization system of first order and ends with the upwind system of second order.

After setting all necessary input conditions, the problem is set to iterate for 1000 iterations within which it gives well converged according to the set convergence criteria so that we can get accurate results.

2.4. Material Property

For any kind of analysis property are the main things which must be defined before moving further analysis. There are thousands of materials available in the ANSYS environment and if required library is not available in ANSYS directory the new material directory can be created as per requirement.

Table 3. Thermo-physical Properties of Air and Aluminium

Properties	Air	Absorber plate (Aluminium)
Density, 'ρ' (Kg/ m ³)	1.225	2719
Specific heat, 'c _p ' (J-Kg/K)	1006.43	871
Thermal conductivity, 'k'(W/ m-K)	0.0242	202.4
Viscosity, 'μ' (N-s/m ²)	1.79×10 ⁻⁵	---
Prandtl number	0.71	---

2.5. Boundary Conditions

For inlet flow to the duct and the outlet flow from the duct is regulated by a uniform velocity inlet boundary state. The air reaches the duct with a uniform velocity at room temperature (T₀ = 300 K) (U₀). The entry velocity of the Reynolds numbers correspond to the various values (3800-15000). A pressure outlet condition with fixed atmospheric pressure of 1.013 × 10⁵ Pa is applied at the exit. Impermeable boundary and slip-free wall conditions over the walls of the duct are applied. At the absorber plate (top wall), the constant flu of 1000 W/m² is given when the under wall is kept in an adiabatic wall. The air temperature inside the duct at the beginning is also 300 K.

III. DATA REDUCTION

The purpose of the present work of CFD is to research the impact that a rib shape has on average Nusselt numbers as well as average friction factor, and THPPs on the underside of the absorber plate in artificially roughened solar air heaters with transverse ribs in squares and X sections.

The average Nusselt number for artificially roughened solar air heaters is defined as:

$$Nu = \frac{h D_h}{K_a}$$

Reynolds number is defined as:

$$Re = \frac{\rho u D_h}{\mu}$$

where ρ is the density of the air inlet, u is the average velocity of the air inlet, D_h is the hydraulic diameter of the wedge duct inlet, and μ is the dynamic viscosity of air at the inlet.

For artificial solar air heaters the average friction factor is determined by:

$$f_r = \frac{(\frac{\Delta P}{L}) D}{2\rho U^2}$$

Where ΔP is pressure drop across the duct of an artificially roughened solar air heater.

The Nusselt number ratio, Nu_{rib}/Nu_s , defined as a ratio of average Nusselt number of rib channel to average Nusselt number of smooth channel. Nu_s represents Nusselt number for smooth duct of a solar air heater and can be obtained by the Dittus–Boelter equation (McAdams 1942):

$$\text{Dittus – Boelter equation } Nu_s = 0.023 Re^{0.8} Pr^{0.4}$$

f_s represents friction factor for smooth duct of a solar air heater and can be obtained by Blasius equation (Fox, Pritchard, and McDonald 2010).

$$\text{Blasius equation } f_s = 0.0791 Re^{-0.25}$$

PEC represents **Performance Evaluation Criteria** of a solar air heater and can be obtained by:

$$PEC = (Nu_r / Nu_s) / (f_r / f_s)^{1/3}$$

IV. RESULTS AND DISCUSSIONS

4.1. CFD validation

Comprehensive and very settled results are promised in computational models. Numerical models of physical dimensions need to be checked, however. The simulation of artificially roughened solar air heaters is conducted with the objective of validating the numerical model, and the results are correlated with the data from **Anil Singh Yadav and J.L. Bhagoria (2017)[6]**, who studied the influence of square rib on rectangular roughened frictional factors and heat transfer.

➤ For $Re = 3800$

The air reaches the duct with a uniform velocity at $Re=3800$ at room temperature $T_0 = 300$ K. A pressure outlet condition with fixed atmospheric pressure of 1.013×10^5 Pa is applied at the exit. At the absorber plate (top wall), the constant flu of 1000 W/m²

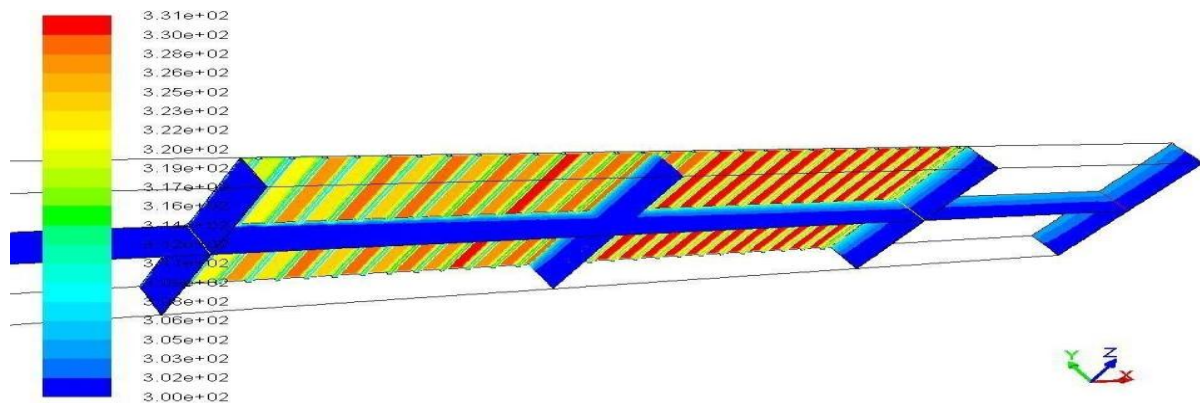


Fig.-5: Temperature contour of square rib section channel of SAH at $Re=3800$.

By way of CFD analysis, the value of the **Nusselt number ratio**, **Friction factor ratio**, and **Performance Evaluation Criteria (PEC)** has been measured at a different Reynold’s number. In contrast with values derived from analyses by **Anil Singh Yadav and J.L. Bhagoria (2017)[6]** the values in the **Nusselt number ratio**, **Friction factor ratio**, and **Performance Evaluation Criteria (PEC)** estimates of the CFD modelling were compared.

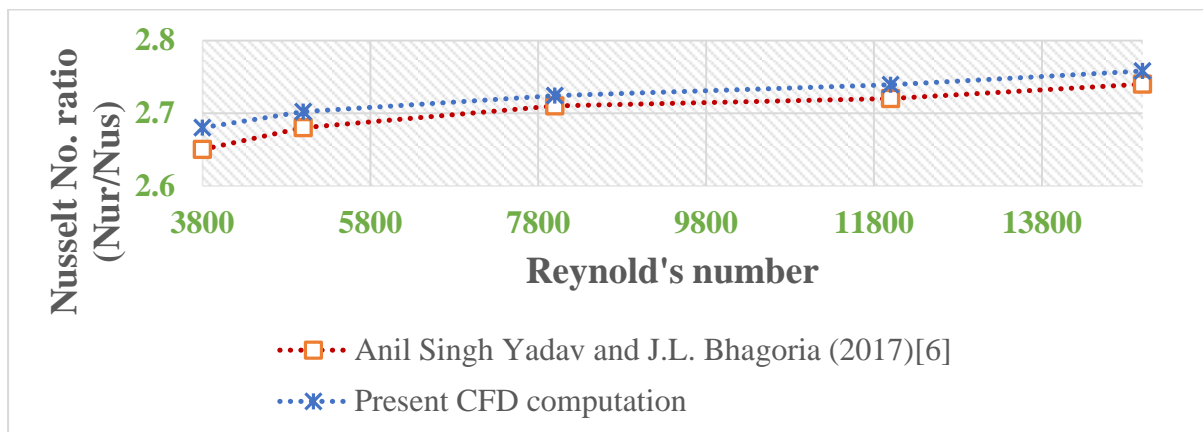


Fig.-6: Comparison of the Nusselt number ratio derived from CFD results and the Anil Singh Yadav and J.L. Bhagoria (2017) [6] results.

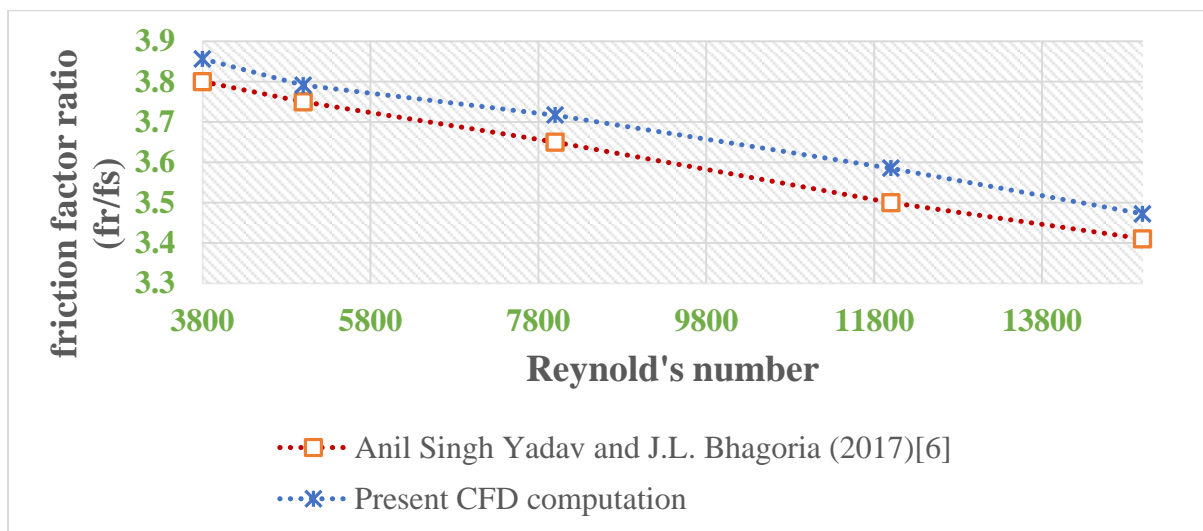


Fig.-7: Comparison of the friction factor ratio derived from CFD results and the Anil Singh Yadav and J.L. Bhagoria (2017) [6] results.

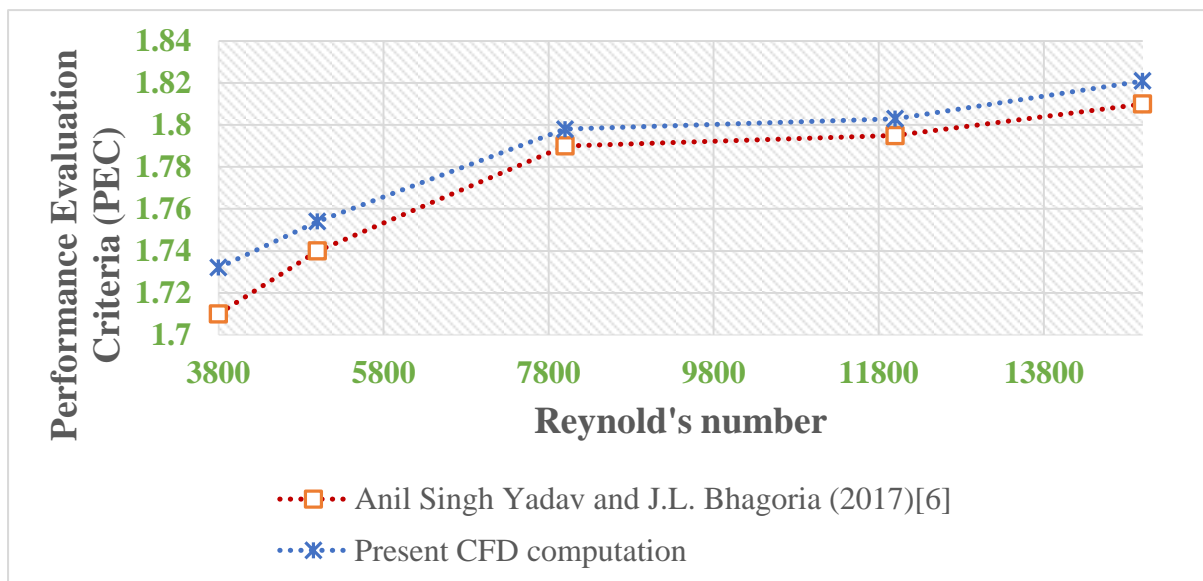


Fig.-8: Comparison of the Performance Evaluation Criteria (PEC) derived from CFD results and the Anil Singh Yadav and J.L. Bhagoria (2017) [6] results.

From the above graph, it is found that the value of **Nusselt number ratio**, **Friction factor ratio**, and **Performance Evaluation Criteria (PEC)** calculated from numerical analysis is closer to value of **Nusselt number ratio**, **Friction factor ratio**, and **Performance Evaluation Criteria (PEC)** obtained from the base paper, which means that numerical model is correct.

4.2. Effect of X-shaped ribs on value of Nusselt number ratio, Friction factor ratio, and Performance Evaluation Criteria (PEC)

CFD computations of heat transfer and fluid flow characteristics in an artificially roughened solar air heater provided with X-sectioned transverse rib roughness on the underside of the absorber plate are performed. The effects of grid density, Reynolds number, on the average heat transfer and friction characteristics for flow of air in an artificially roughened solar air heater are discussed in the following sub-sections.

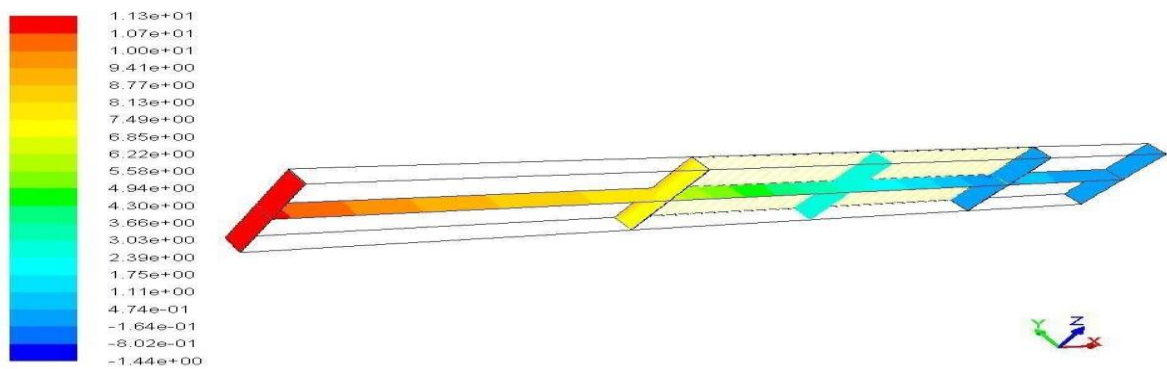


Fig.-9: Pressure contour of X-shape rib section channel of SAH at Re=3800.

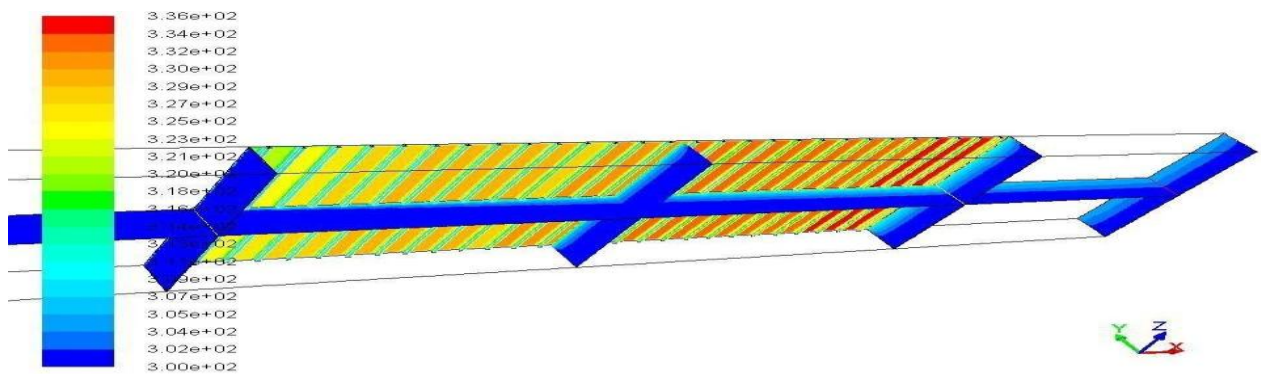


Fig.-10: Temperature contour of X-shape rib section channel of SAH at Re=3800.

4.3. Comparison between the value of the Nusselt number ratio, Friction factor ratio, and Performance Evaluation Criteria (PEC) for Square and X-shaped rib on the absorber plate

To improve previous understandings and to distinct the contribution of providing a X-shaped ribs to the overall thermal enhancement of proposed design, absorber plate with square and X-shaped ribs on the absorber plate are compared in this section.

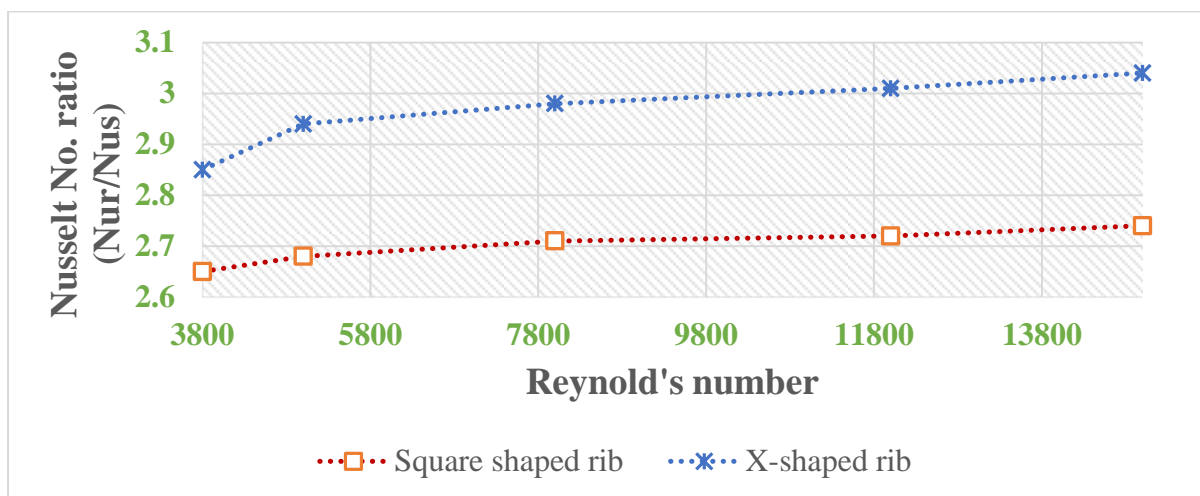


Fig.-11: Comparison of the Nusselt number ratio values with square and X-shaped ribs on the absorber plate.

Figure 11. Shows the variation of Nusselt number ratio (enhancement ratio) as a function of Reynolds number and for fixed value of relative roughness height of 0.042. In this case, the Nusselt number ratio increases with increase in Reynold’s number for all the cases.

The maximum enhancement in Nusselt number is found to be in X-shaped ribs, which is 1.109 times that of square ribs corresponding to at a Reynolds number of 15,000 for the investigated range of parameters.

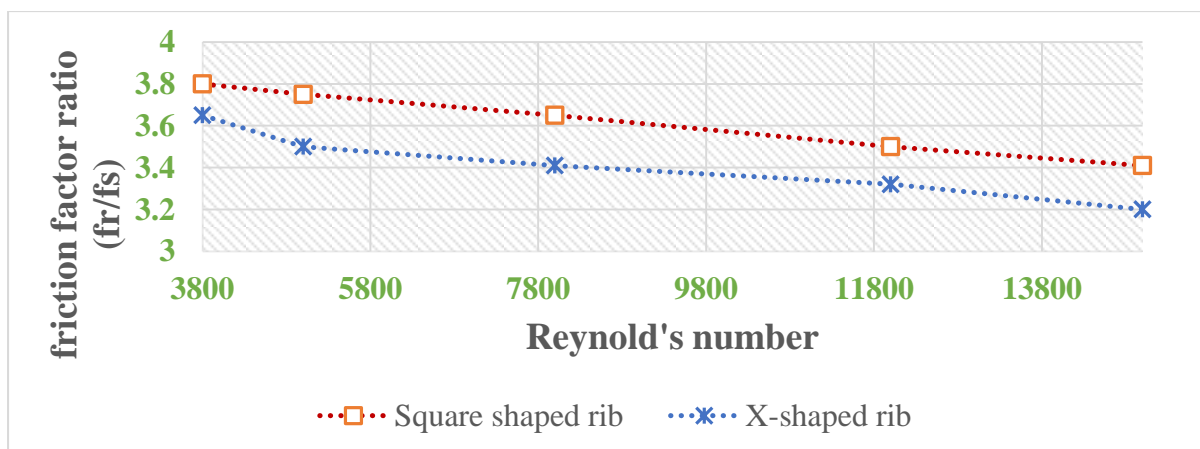


Fig.-12: Comparison of the friction factor ratio values with square and X-shaped ribs on the absorber plate.

Figure 12 shows the variation of friction factor ratio (enhancement ratio) as a function of Reynolds number and for fixed value of relative roughness height of 0.042. In this case, the friction factor ratio decreases with increase in Reynold’s number for all the cases.

The minimum friction factor ratio is found to be in X-shaped ribs, which is 0.938 times that of square ribs corresponding to at a Reynolds number of 15,000 for the investigated range of parameters.

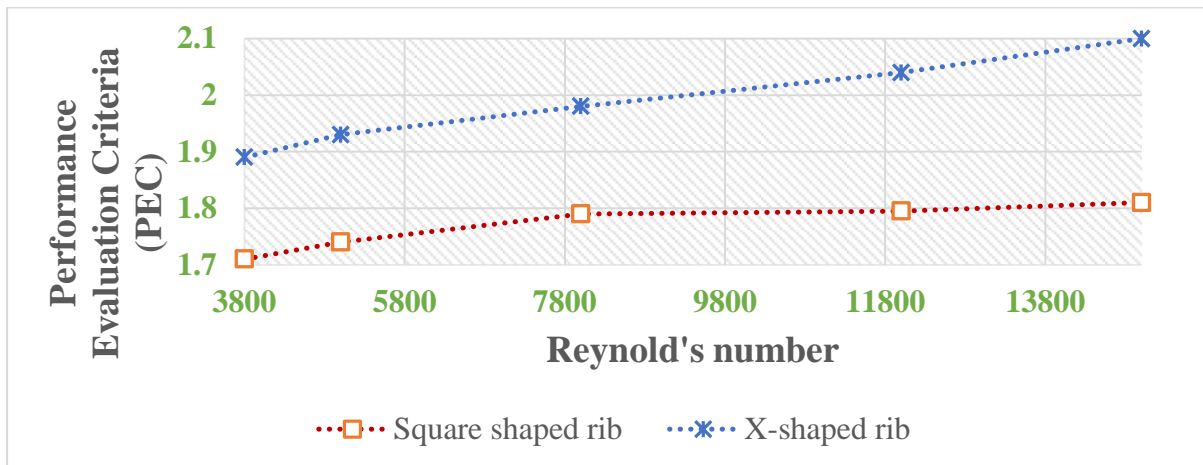


Fig.-13: Comparison of the Performance Evaluation Criteria (PEC) values with square and X-shaped ribs on the absorber plate.

V. CONCLUSIONS

Based on the CFD provision currently in operation, the following related results can be reached by analyzing a 3D solar air heater with square and X-sections transverse rib roughness on the absorber plate with the heat transfer and flow friction, the following conclusions can be drawn:

- The maximum enhancement in **Nusselt number** is found to be in X-shaped ribs, which is 1.109 times that of square ribs corresponding to at a Reynolds number of 15,000 for the investigated range of parameters.
- The minimum **friction factor ratio** is found to be in X-shaped ribs, which is 0.938 times that of square ribs corresponding to at a Reynolds number of 15,000 for the investigated range of parameters.
- The maximum enhancement in **Performance Evaluation Criteria (PEC)** is found to be in X-shaped ribs, which is 1.160 times that of square ribs corresponding to at a Reynolds number of 15,000 for the investigated range of parameters.
- The solar air heater with X-sectioned rib roughness on the absorber plate has been found to yield improved results relative to the square sectioned transverse rib and can thus be used to increase the heat transfer.

VI. REFERENCES

- [1] Alam, T., and M. H. Kim. 2017. A critical review on artificial roughness provided in rectangular solar air heater duct. *Renewable and Sustainable Energy Reviews* 69:387–400. doi:10.1016/j.rser.2016.11.192.
- [2] Kalogirou, S. A., S. Karellas, K. Braimakis, C. Stanciu, and V. Badescu. 2016. Exergy analysis of solar thermal collectors and processes. *Progress in Energy and Combustion Science* 56:106–37. doi:10.1016/j.pecs.2016.05.002.
- [3] Sharma, S. K., and V. R. Kalamkar. 2015. Thermo-hydraulic performance analysis of solar air heaters having artificial roughness-A review. *Renewable and Sustainable Energy Reviews* 41:413–35. doi:10.1016/j.rser.2014.08.051.
- [4] Arunkumar, H. S., K. V. Karanth, and S. Kumar. 2020. Review on the design modifications of a solar air heater for improvement in the thermal performance. *Sustainable Energy Technologies and Assessments* 39:100685. doi:10.1016/j.seta.2020.100685.
- [5] Gabhane, M. G., and A. B. Kanase-Patil. 2017. Experimental analysis of double flow solar air heater with multiple C shape roughness". *Solar Energy* 155:1411–16. doi:10.1016/j.solener.2017.07.038.

- [6] Anil Singh Yadav & J.L. Bhagoria (2017) Numerical investigation of flow through an artificially roughened solar air heater, *International Journal of Ambient Energy*, 36:2, 87-100, DOI: 10.1080/01430750.2013.823107
- [7] Alam, T., R. P. Saini, and J. S. Saini. 2014. Effect of circularity of perforation holes in V-shaped blockages on heat transfer and friction characteristics of rectangular solar air heater duct. *Energy Conversion and Management* 86:952–63. doi:10.1016/j.enconman.2014.06.050.
- [8] Al-Dabaggah, M., Z. A. H. Obaid, M. Al Qubeissic, D. Dixon-Hardy, J. Cottome, and P. J. Heggssd. 2015. CFD modeling and performance evaluation of multipass solar air heaters. *Numerical Heat Transfer, Part A: Applications* 76 (6):438–64. doi:10.1080/10407782.2019.1637228.
- [9] Poongavanam, G. K., K. Panchabikesan, A. J. D. Leo, and V. Ramalingam. 2018. Experimental investigation on heat transfer augmentation of solar air heater using shot blasted V-corrugated absorber plate. *Renewable Energy* 127:213–29. doi:10.1016/j.renene.2018.04.056.
- [10] Yang, Y., and P. Chen. 2014. Numerical study of a solar collector with partitions. *Numerical Heat Transfer, Part A: Applications* 66 (7):37–41. doi:10.1080/10407782.2014.892330.
- [11] Gilani, S. E., H. H. Al-Kayiem, D. E. Woldemicheal, and S. I. Gilani. 2017. Performance enhancement of free convective solar air heater by pin protrusions on the absorber. *Solar Energy* 151:173–85. doi:10.1016/j.solener.2017.05.038.
- [12] Priyam, A. 2017. Heat transfer and pressure drop characteristics of wavy fin solar air heater. *International Journal of Heat and Technology* 35 (4):1015–22. doi:10.18280/ijht.350438.
- [13] Yadav, K. D., and R. K. Prasad. 2020. Performance analysis of parallel flow flat plate solar air heater having arc shaped wire roughened absorber plate. *Reinforced Plastics* 32:23–44. doi:10.1016/j.ref.2019.10.002.
- [14] Thakur, S., and N. S. Thakur. 2020. Impact of multi-staggered rib parameters of the 'W' shaped roughness on the performance of a solar air heater channel. *Energy Sources, Part A: Recovery, Utilization, and Environmental Effects* 1–20. doi:10.1080/15567036.2020.1764672.
- [15] Wang, L., and B. Sunden. 2007. Experimental investigation of local heat transfer in a square duct with various-shaped ribs. *Heat and Mass Transfer* 43 (8):759–66. doi:10.1007/s00231-006-0190-y.
- [16] Webb, R. L., and E. R. Eckert. 1972. Application of rough surfaces to heat exchanger design. *International Journal of Heat and Mass Transfer* 15 (9):1647–58. doi:10.1016/0017-9310(72)90095-6.
- [17] Yadav, A. S., and J. L. Bhagoria. 2013a. A CFD (computational fluid dynamics) based heat transfer and fluid flow analysis of a solar air heater provided with circular transverse wire rib roughness on the absorber plate. *Energy* 55:1127–42. doi:10.1016/j.energy.2013.03.066.
- [18] Yadav, A. S., and J. L. Bhagoria. 2013b. Heat transfer and fluid flow analysis of solar air heater: A review of CFD approach. *Renewable and Sustainable Energy Reviews* 23:60–79. doi:10.1016/j.rser.2013.02.035.
- [19] Yadav, A. S., and J. L. Bhagoria. 2014a. A numerical investigation of square sectioned transverse rib roughened solar air heater. *International Journal of Thermal Sciences* 79:111–31. doi:10.1016/j.ijthermalsci.2014.01.008.
- [20] Yadav, A. S., and J. L. Bhagoria. 2014b. A numerical investigation of turbulent flows through an artificially roughened solar air heater. *Numerical Heat Transfer, Part A: Applications* 65 (7):679–98. doi:10.1080/10407782.2013.846187.
- [21] Yadav, A. S., and J. L. Bhagoria. 2014c. A CFD based thermo-hydraulic performance analysis of an artificially roughened solar air heater having equilateral triangular sectioned rib roughness on the absorber plate. *International Journal of Heat and Mass Transfer* 70:1016–39. doi:10.1016/j.ijheatmasstransfer.2013.11.074.